THE ASTROPHYSICAL JOURNAL, 509:L129–L132, 1998 December 20

ACOUSTIC SIGNATURES OF SUBPHOTOSPHERIC STRUCTURE UNDERLYING SUNSPOTS

C. LINDSEY AND D. C. BRAUN[1]
Solar Physics Research Corporation, 4720 Calle Desecada, Tucson, AZ 85718
Received 1998 July 9; accepted 1998 September 30; published 1998 November 11

ABSTRACT

Helioseismic holography of active regions at frequencies in the range of 5–6 mHz renders acoustic signatures that we think signify acoustic perturbations several megameters beneath the photosphere. The application of holographic diagnostics at 5–6 mHz gives us images with considerably finer horizontal spatial resolution, and likewise much finer depth resolution with respect to focus, than the 3 mHz diagnostics we have recently published. This Letter reports comparative results of standard focus-defocus diagnostics of a single sunspot at 3 and 6 mHz. Images of the "acoustic egression power" at 6 mHz show a remarkable, compact acoustic deficit that persists in acoustic focal planes submerged up to 11.2 Mm beneath the solar surface. We propose that this and other similar features associated with other active regions are the result of refraction or scattering by submerged thermal or Doppler perturbations of an acoustic deficit that is caused by strong wave absorption in the overlying photosphere of the active region.

Subject headings: Sun: activity — Sun: oscillations — sunspots

1. INTRODUCTION

Over the late 1980s and 1990s, we have developed a diagnostic called "helioseismic holography" (Lindsey & Braun 1990, 1997; Braun et al. 1992). This analysis treats helioseismic observations over the solar surface computationally in a way that is entirely analogous to how the eye treats the electromagnetic field it samples at the surface of the cornea. The foregoing references define helioseismic holography in terms of seismic imaging by the "acoustic reconstruction" of the solar interior acoustic field based on observations of the disturbance it creates at the solar surface. The recent advent of the *Solar and Heliospheric Observatory* (*SOHO*) and the Global Oscillation Network Group now gives us the high-resolution, helioseismic observations needed for this diagnostic.

The basic technique is illustrated by Lindsey & Braun (1997) using artificial data. Braun et al. (1998) and Lindsey & Braun (1998a, 1998b) applied the diagnostic to *SOHO*/Michelson Doppler Imager (MDI) observations, making a number of remarkable discoveries. The purpose of this Letter is to report two notable developments. The first is helioseismic images at the higher acoustic frequencies, 5–6 mHz, which show clear signatures of acoustic perturbations thousands of kilometers beneath active-region photospheres. These signatures are, in fact, quite common in large active-region complexes and suggest a physical structure beneath active regions that is actually quite interesting and not by any means entirely predictable. The second is the resolution of an important technical problem encountered by Braun et al. (1998), called the "focus anomaly," which heretofore presented an encumbrance to reliable helioseismic depth diagnostics. We will first discuss the focus anomaly and its resolution. We will then present our first significant encounter with the diagnostic signature of an acoustic perturbation that we are convinced lies several megameters beneath the solar surface. We will begin with a brief review.

[1] Also High Altitude Observatory (HAO), National Center for Atmospheric Research, P.O. Box 3000, Boulder, CO 80307-3000. The National Center for Atmospheric Research is sponsored by the National Science Foundation.

2. REVIEW

As an interior diagnostic, helioseismic holography can be understood by considering its application to the wave pattern that is created at the solar surface by a single, submerged monopolar point source. Helioseismic measurements of the surface disturbance are applied in time reverse to the surface of a quiet solar model, so as to excite waves into the model interior that are the time reverse of those emanating from the source. Helioseismic holography acoustically regresses the resulting wave pattern back into the solar interior model, where it reconverges to render an image of the source. In fact, this procedure will render any distribution of sources in the case of an arbitrarily complex source configuration. If the said quiet solar model is sampled over a surface that rests at the depth of a particular source that gave rise to the observed disturbance, the image of that particular source is rendered sharp. Placement of the "focal plane" below or above the appropriate source depth results *not* in a disappearance of the image but simply in a defocusing of the image. This offers a powerful depth diagnostic that we will demonstrate herein.

Helioseismic holography makes no attempt to incorporate the physical perturbations that give rise to the surface acoustic signature into the quiet solar model to which the time-reverse disturbance has been applied. Since this model is specifically devoid of any such perturbations, the Born approximation becomes implicit. In practice, this simply requires that a substantial fraction of acoustic radiation emanating from a particular source in the actual solar interior must arrive at the solar surface without undergoing a further significant scattering by some intervening acoustic perturbation. This condition is analogous to that which generally applies in familiar electromagnetic optics, which makes no attempt to reconstruct informative images from radiation that has passed through a shower glass, or thick clouds, for instance.

The basic formalism that expresses the image amplitude at any particular point in the focal plane is a coherent integral over a region on the solar surface called the computational "pupil" (see eq. [10] in Lindsey & Braun 1997). We call this

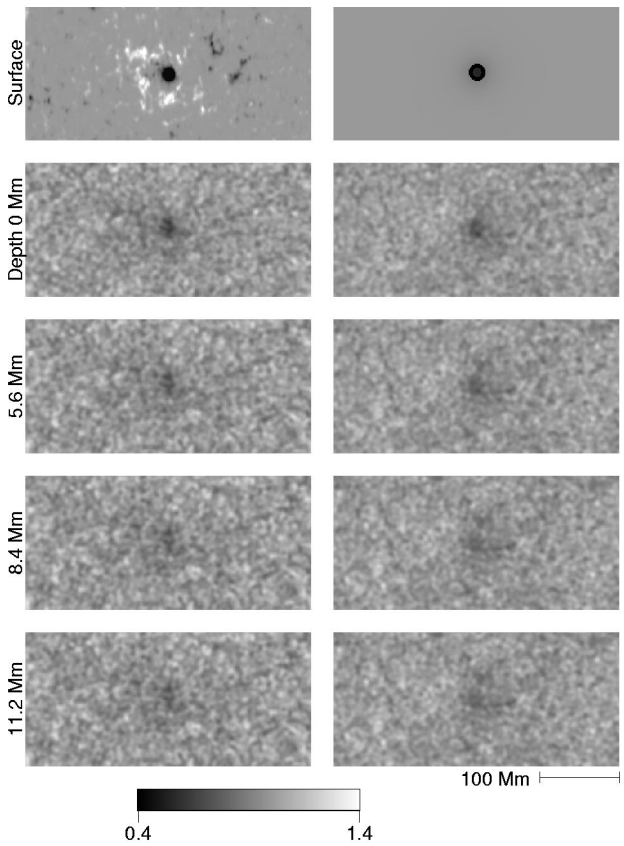

FIG. 1.—Egression-power images of *SOHO*/MDI observations of NOAA AR 7973 (1996 June 25.0–26.0) are computed in a 1 mHz bandpass centered at 3 mHz at various depths (*left column*) so as to be compared with egression-power images similarly computed from model computations based on simulated random noise (*right column*). Random noise is introduced into the atmosphere of Christensen-Dalsgaard et al. and propagated back to the surface, whereupon the egression computation is applied. The top frame on the left shows the concurrent Kitt Peak magnetogram of NOAA AR 7973. The upper right frame shows the absorption map applied to the noise at the surface of the model. The linear gray scale at the bottom of the figure applies to all of the egression-power images in both columns, normalized to unity by dividing the egression (eq. [1]) by its time-reversed counterpart, the *in*gression, defined by Lindsey & Braun (1997).

integral the "egression":

$$H_+(z, \mathbf{r}, t) = \int dt' \int_{a<|\mathbf{r}-\mathbf{r}'|<b} d^2\mathbf{r}'\psi(\mathbf{r}', t') \times G_+(z, \mathbf{r}, t, \mathbf{r}', t'), \quad (1)$$

where G_+ is the Green's function that propagates the observed surface disturbance, represented by ψ, as a source, backward into the solar interior. The egression has its analogy in the *Kirchhoff integral* of wave optics for a uniform medium (see Born & Wolf 1975, eq. [13]). The formal Kirchhoff integral has two propagating terms, which are distinguished by the application of temporal and spatial derivatives of ψ. The egression neglects these distinctions, collapsing into the single integral expressed above. In our application, the computation is confined to an annular pupil surrounding the point $\mathbf{r}$ whose inner radius is a and whose outer radius is b.

For what we call simple "single-skip holography," G_+ is understood to be the "single-skip Green's function," representing only waves that propagate from a source to encounter the surface for the first time, whereupon they are supposed to register an observable disturbance and disappear without being reflected. This can actually be regarded as an accurate representation of the Green's function in its entirety for frequencies above approximately 4.5 mHz, where the solar surface acts as an efficient absorber. Below this frequency, the photosphere is an efficient specular reflector, and it is then important to distinguish between the Green's function in its entirety and that component of the Green's function which we will call the "*n*-skip Green's function," representing the transient disturbance that has skipped to the surface exactly *n* times and no less since leaving the source. The diagnostic employed here is simple acoustic power holography, in which the egression is simply squared and integrated over time.

The MDI instrument and its data products are described in some detail by Scherrer et al. (1995). The MDI Dopplergrams of NOAA Active Region 973 cover the full solar disk with a pixel spacing of 2″. The Dopplergrams to which we applied the computations described above were made with a 1 minute cadence over a 24 hr period.

3. DEPTH DIAGNOSTICS

Depth diagnostics that are based on the defocusing of the acoustic egression image as the focal plane is submerged suggest that the acoustic perturbations representing the sunspot in NOAA AR 7973 at 3 mHz are superficial. Braun et al. (1998) compared egression images of a single sunspot and surrounding acoustic moat with control computations of a model atmosphere driven by random noise that was introduced locally over the surface of the model. The defocus profiles of the egression power maps they obtained from the MDI observations fitted their respective model profiles poorly, clearly indicating the need for an improved model. It now appears that this "focus anomaly" can be explained entirely by the neglect in their noise model of image smearing, an attribute intentionally designed into the MDI instrument in order to suppress aliasing. How this smearing contrives to render images that defocus more rapidly with focal-plane depth than unsmeared images is somewhat subtle, and we do not attempt an explanation here. However, with the noise models of Braun et al. (1998) appropriately smeared, the comparative egression computations fall into close agreement with those made from the MDI observations.

This is illustrated in Figure 1, which compares egression-power images of NOAA AR 7973 (*left column*) with egression-power images of a model (*right column*) in which random noise is introduced into the atmosphere of Christensen-Dalsgaard, Proffitt, & Thompson (1993). The top image in the left column is a magnetogram of NOAA AR 7973. The underlying images in the left column show 3 mHz egression-power images of the region for depths up to 11.2 Mm. These images clearly show the local egression-power deficit that is expected from the strong absorption of acoustic waves by the sunspot (Braun, Duvall, & LaBonte 1988). The top image on the right shows a map of local acoustic absorption that was applied at the surface of the noise model. The noise was propagated a single skip into the model interior and back to the surface, and the resultant surface disturbance was analyzed in the same fashion as the *SOHO* observations in order to render the egression images stacked in the underlying right column. The acoustic emission profile shown in the upper right frame was fashioned to fit the egression signature of the sunspot at a depth of zero, which was obtained from the MDI observations as closely as possible.

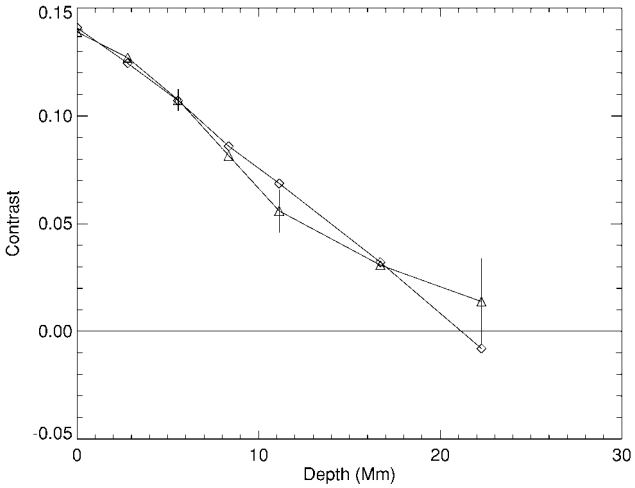

FIG. 2.—Contrasts of the sunspot acoustic deficits of the images in Fig. 1 are plotted as a function of depth. The egression power in each image was averaged over a disk of radius 8.4 Mm and over the immediately outlying annulus with a radius of 12.6 Mm. The difference between these two averages was normalized to the latter. The triangles represent MDI sunspot egression contrasts. The diamonds represent the same for the model.

Comparative contrast measurements of the egression-power signatures imaged in Figure 1 are plotted in Figure 2. Here the egression power in each image was averaged over a disk of radius 8.4 Mm and over the immediately outlying annulus with outer radius 12.6 Mm. The difference between these two averages was normalized to the latter. The triangles represent MDI egression contrasts. The diamonds represent the same for the model. The reader should note that this scheme measures only the high-resolution contrast of the sunspot signature itself, within 8.4 Mm of its center, with respect to its near surrounding. The egression-power contrast of the sunspot with respect to the quiet Sun 50 Mm outside of the sunspot is much greater, ~50%, but the major contributors to this contrast are components, such as the acoustic moat, that are spatially more extended and therefore respond fairly sluggishly to the submergence of the focal plane.

4. THE 5–6 mHz DEPTH DIAGNOSTICS

The advantages of depth diagnostics at higher frequencies are considerable. Where depth discrimination by defocus is the proposition, the horizontal scale of the object is critical. Large fuzzy smears defocus more sluggishly than small sharp features. Diffraction smears images, limiting the sharpness with which defocus renders the object vertically localized. Figure 3 illustrates this with the same active region as imaged in Figure 1. The egression-power image of the sunspot at 6 mHz is considerably sharper than that at 3 mHz (Fig. 1) and sits inside of a somewhat elliptical "acoustic penumbra" that is actually considerably more extensive than the white-light penumbra, visible in the image at top left, but not nearly as extensive as the acoustic moat, seen in 3 mHz egression-power maps (Braun et al. 1998; Lindsey & Braun 1998a). The center of the sunspot is represented by a strong acoustic deficit signature, but immediately to its left, indicated by an arrow in the left column of frames, is a "satellite," a compact egression deficit signature that lies clear outside of the white-light penumbra of the sunspot.

As the focal plane of the egression computation is submerged, the acoustic deficit signature representing the sunspot

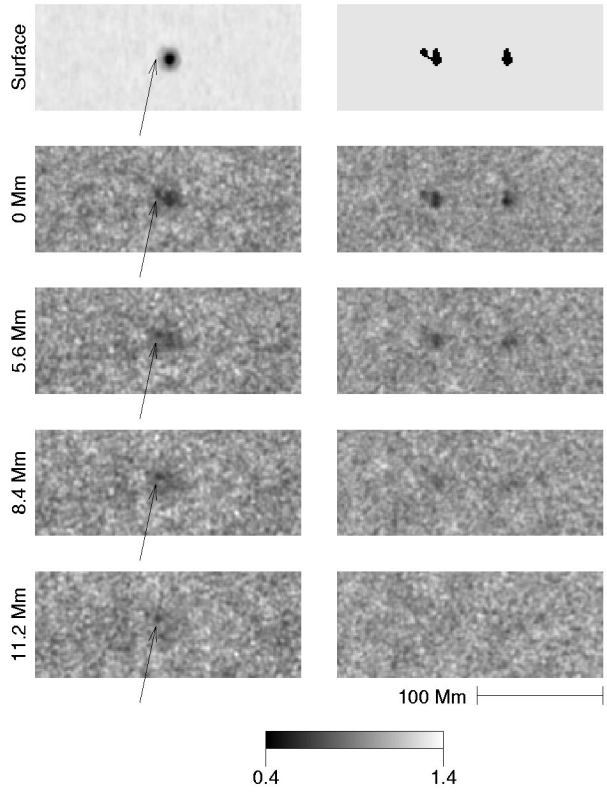

FIG. 3.—Egression-power images of *SOHO*/MDI observations of NOAA AR 7973 (1996 June 25.0–26.0) are computed in a 1 mHz bandpass centered at 6 mHz. Again, the left column shows egression images of MDI observations, while the right column shows egression images of a model. The top frame on the left shows the concurrent Kitt Peak visible continuum image of NOAA AR 7973. The upper right frame shows the absorption map applied to the noise at the surface of the model. The arrows in the left frames locate a compact satellite that appears clear outside of the white-light penumbra of the sunspot and persists to focal planes 11.2 Mm in depth. The linear gray scale at the bottom of the figure applies to all of the egression-power images in both columns, normalized to unity for the mean quiet Sun.

itself defocuses rapidly (*left column*). However, the signature of the satellite in the MDI image persists to a depth of approximately 11.2 Mm with an amplitude of 0.25 (4.1 σ) before fading. This is the first instance we have encountered of a signature that requires a significant acoustic perturbation thousands of kilometers beneath the solar photosphere.

The right column in Figure 3 shows comparative egression-power images of an acoustic-noise model analogous to that in the right column of Figure 1, one in which the absorption of *both sunspot and satellite* are superficial. The absorption profile of this model (*upper right frame, left of frame center*) is tailored to fit the egression-power signature of the sunspot and satellite at zero depth. At the right of frame center, just the sunspot is represented, without the satellite. A careful comparison of the signatures in the left column with those in the right column shows a primary sunspot image in the left column that defocuses at a rate roughly the same as does the primary sunspot image to the right of frame center in the right column. The image of the satellite in the left column, however, persists to a significantly greater depth than its counterpart left of frame center in the right column.

What is most significant in this comparison is *not* that the satellite in the MDI egression-power image persists to a greater depth than the model. Our experience with the focus anomaly described by Braun et al. (1998) reminds us that models can

be treacherous. However, we cannot conceive of any scheme whereby the egression-power signature of the satellite would persist to a significantly *greater* depth than that of the primary sunspot signature in a subphotosphere in which the acoustic perturbations that gave rise to both were entirely superficial. The example shown in Figure 3 is no longer unique. Follow-up analyses of other active regions, and active-region complexes, reported by Braun & Lindsey (1998) have now provided us with a number of egression-power signatures that appear in focal planes up to 20 Mm beneath the solar surface. These "condensations" need not have a significant counterpart near the surface.

To summarize, then, most of the signatures we have encountered in egression-power images of solar activity over the range of 3–6 mHz appear to be consistent with local acoustic perturbations that are superficial. These include the primary acoustic images of sunspots and plages over the entire 3–6 mHz range and the acoustic moats, which appear in 3–4 mHz images. However, there commonly appear signatures in 5–6 mHz egression-power images of active regions, particularly large active-region complexes, that we think can only be explained by acoustic perturbations that are many megameters beneath the solar photosphere.

5. DISCUSSION AND CONCLUSIONS

We believe that the results reported herein, and the forthcoming examples presented by Braun & Lindsey (1998), comprise compelling evidence for the existence of strong acoustic perturbations 10 Mm beneath the solar photosphere. Chang et al. (1997) were the first to apply helioseismic holography to actual solar observations, computing egression-power images of NOAA AR 7973 (the same active region that we have imaged in this study) from observations by the Taiwan Oscillation Network (TON). They claim that their images establish a strong absorption of *p*-modes up to 40 Mm directly beneath the sunspot. Based on criticism by Braun et al. (1998), we believe that these signatures, which Chen et al. (1998) now invariably see directly beneath all large sunspots, are simply the defocused images of acoustic absorption that is superficial. That these signatures remain invariably stationary as the focal plane is submerged strongly suggests this. The analyses of Chang et al. (1997) and Chen et al. (1998) lack the basic control work needed to assess how their egression-power signatures *should* extend in depth for perturbations that *are* superficial. The results presented herein and by Braun & Lindsey (1998) suggest a reality entirely different from the acoustic stalactites that Chang et al. (1997) and Chen et al. (1998) claim are beneath all sunspots. Most of the acoustic signatures seen in our images are consistent with an acoustic deficit that is of entirely superficial origin, defocusing as the focal plane submerges at a rate commensurate with control computations of models representing superficial absorbers. The condensations that appear in deeply submerged focal planes show a limited regard for the locations of overlying sunspots at the surface.

A major question that needs to be addressed, given that the condensations are a result of deep subsurface acoustic perturbations, is the physical character of the supposed interaction between these perturbations and the acoustic waves that represent them at the solar surface. Such perturbations require considerable damping or scattering forces to render the acoustic deficits shown by the egression-power maps. It appears to us that magnetic forces themselves are not a plausible candidate for such a mechanism. Lindsey et al. (1996) argue that magnetic scattering at depths greater than 5 Mm by magnetic fluxes typical of a large sunspot would be insignificant. In fact, the forces required for significant damping are similar to those required for scattering, and so the same argument applies. We suggest that the acoustic condensations are the signature of submerged thermal or Doppler perturbations that simply scatter an acoustic deficit that originates at the overlying solar surface, where actual wave absorption is efficient. This is what Braun et al. (1998) and Lindsey & Braun (1998a) suggest for the superficial acoustic deficit that represents what they call the "acoustic moat" surrounding sunspots in 3 mHz egression-power images of active regions. The phase-sensitive holography described by Lindsey & Braun (1997) is designed to render subsurface refractive or Doppler perturbations that are not fortunate enough to be illuminated by a nearby surface acoustic absorber. This will probably give us some insight into the acoustics that give rise to these features.

We greatly appreciate the excellent support our research has gotten from the *SOHO*/MDI team and the fine quality of the helioseismic data that they have given us. We especially appreciate Tom Duvall's long-term cooperation with our research effort. We also appreciate Tom Bogdan's prompt and thorough review of the manuscript at our request. D. C. B., a long-term visitor at the HAO, is grateful to Michael Knölker and the staff of the HAO for their hospitality and support. This research was supported by NSF grants ATM 9214714, AST 95-21637, and AST 95-28249 and by NASA grant NAGW-97029.

REFERENCES

Born, M., & Wolf, E. 1975, Principles of Optics (Oxford: Pergamon), 378
Braun, D. C., Duvall, T., & LaBonte, B. J. 1988, ApJ, 335, 1015
Braun, D. C., & Lindsey, C. 1998, ApJ, submitted
Braun, D. C., Lindsey, C., Fan, Y., & Fagan, M. 1998, ApJ, 502, 968
Braun, D. C., Lindsey, C., Fan, Y., & Jefferies, S. M. 1992, ApJ, 392, 739
Chang, H.-K., Chou, D.-Y., & LaBonte, B. J., & the TON Team. 1997, Nature, 389, 825
Chen, H.-R., Chou, D.-Y., Chang, H.-K., Sun, M.-T., Yeh, S.-J., LaBonte, B. J., & the TON Team. 1998, ApJ, 501, L139
Christensen-Dalsgaard, J., Proffitt, C. R., & Thompson, M. J. 1993, ApJ, 403, L75
Lindsey, C., & Braun, D. C. 1990, Sol. Phys., 126, 101
———. 1997, ApJ, 485, 895
———. 1998a, ApJ, 499, L99
———. 1998b, ApJ, in press
Lindsey, C., Braun, D. C., Jefferies, S. M., Woodard, M. F., Fan, Y., Gu, Y., & Redfield, S. 1996, ApJ, 470, 636
Scherrer, P. H., et al. 1995, Sol. Phys., 162, 129